

Supporting Information

Structures and Anti-cancer Properties of Two Binuclear Copper Complexes

Xiu Ying Qin ^{a,b}, Li Cong Yang ^a, Fang Ling Le ^a, Qian Qian Yu ^a, Dong Dong Sun ^a, Ya Nan Liu ^c, Jie Liu ^{*a}

^a Department of Chemistry, Jinan University, Guangzhou 510632, China. Fax: 86 20 85221263; Tel: 86 20 85220223; E-mail: tliuliu@jnu.edu.cn

^b College of Pharmacy, Guilin Medical University, Guilin, China.

^c Department of Biology, The Chinese University of Hong Kong, Hong Kong, China.

Experimental Procedures

Instruments

IR spectras were taken on a Pekin-Elmer spectrum One FT-IR spectrometer with KBr pallets in the range of 4000~400 cm⁻¹. The elemental analyses for C, H and N were performed on a Perkin-Elmer 2400C elemental analyzer. The crystal structures were determined by a Bruker Breeze CCD area detector. Apoptosis assays were determined by BD FACSCalibur, and cellular uptake and the levels of reactive oxygen species were determined both by Zeiss Confocal Laser Scanning Microscope (LSM-510) and by BD FACSCalibur.

Materials

Both solvents and chemicals obtained from commercial sources were of reagent grade and used without further purification unless specially noted. Cell culture: Cells were cultured in DMEM medium supplemented with heat inactivated fetal bovine serum (FBS, 10 %), penicillin (100 µg.mL⁻¹) and streptomycin (100 µg.mL⁻¹). They were incubated at 37°C in a humidified incubator with 5 % CO₂ and 95 % air. The medium was changed thrice weekly.

Cell culture plates (NEST) were used.

Synthesis of Cu-1

A mixed solution containing Cu(CH₃COO)₂·H₂O (0.0998g, 0.5 mmol) and N-(2)-L-alanyl-L-glutamine (0.1086g, 0.5 mmol) in methanol (20 mL) was stirred at 323 K for 4h, its pH value was adjusted to 6.5, and then a solution containing 4,4'-Bipyridine (0.076g, 0.5mmol) was added to the mixed solution. Subsequently, the mixed solution was stirred at 323 K for 1 d, the resulting reagents were filtrated, and the filtrate was left at room temperature. Some blue crystals were obtained after some days, giving blue needle-shaped single crystals that were suitable for X-ray diffraction. For C₂₆ H₅₄ Cu₂ N₈ O₁₈, [Cu₂(C₁₀H₈N₂)(C₈H₁₃O₄N₃)₂(H₂O)₂]₂·8H₂O (Cu-1), anal. calcd, %: C, 34.95; H, 6.11; N,12.52. Found, %: C, 34.94; H, 6.09; N, 12.54. IR (KBr, ν, cm⁻¹): 3407.37, 2972.52, 2934.06, 1659.82, 1587.44, 1492.47, 1420.44, 1304.69, 1225.05, 1097.43, 1072.03, 968.49, 866.99, 818.56, 644.80, 570.70, and 510.35 cm⁻¹ [Fig. S1(a)]. In the IR spectrum of Cu-1, the band at 3407.37 cm⁻¹ is assigned to ν(-OH of water) absorption, and the bands at 2972.52 and 2934.06 cm⁻¹ are assigned to ν(C-H of -CH₃ and -CH₂-) absorption, and the band at 1659.82 cm⁻¹ is assigned to ν(-COO⁻), and the band at 1587.44cm⁻¹ is assigned to ν(-C=N- or -C=C-)

absorption of aromatic ring, and the bands at 644.80 and 570.70 cm^{-1} are assigned to ν (Cu-N and Cu-O) absorption. The crystal productivity is 69.26%, based on N-(2)-L-alanyl-L-glutamine.

Synthesis of Cu-2

2,6-diformyl-4-methylphenol was synthesized according to the references^{1,2}. The Schiff base ligand, namely, N, N-bis(3-formyl-5-methyl-salicylidene)alanine potassium salt [$\text{C}_{15}\text{H}_{15}\text{O}_5\text{N}_2\text{K}_3$, abbreviatedly as $\text{K}_3(\text{SB})_2$], was synthesized according to the references³ by using the raw materials including 2,6-diformyl-4-methylphenol, β -alanine and potassium hydroxide. A mixed solution containing $\text{K}_3(\text{SB})_2$ (0.0842g, 0.2 mmol), 4,4'-bipyridine (0.0308 g, 0.2 mmol) and CuSO_4 (0.0322g, 0.2 mmol) in methanol (20 mL) was stirred at 333 K for 20h. Subsequently, the resulting reagents were filtrated, and the filtrate was left at room temperature. Some green crystals were obtained after some days, giving green columnar-shaped single crystals that were suitable for X-ray diffraction. For $\text{C}_{36}\text{H}_{42}\text{Cu}_2\text{N}_4\text{O}_{12}$, $[\text{Cu}_2(\text{C}_{10}\text{H}_8\text{N}_2)(\text{C}_{12}\text{H}_{11}\text{O}_4\text{N})_2(\text{CH}_3\text{OH})_2] \cdot 2\text{H}_2\text{O}$ (Cu-2), anal. calcd, %: C, 50.82; H, 4.99; N, 6.57. Found, %: C, 50.88; H, 4.98; N, 6.59. IR (KBr, ν , cm^{-1}): 3419.58, 2927.04, 2857.97, 1670.40, 1619.99, 1580.31, 1542.52, 1458.39, 1393.14, 1337.25, 1304.74, 1229.01, 1030.71, 972.06, 649.89, and 530.04 cm^{-1} [Fig. S1(b)]. In the IR spectrum of Cu-2, the band at 3419.58 cm^{-1} is assigned to ν (-OH of water) absorption, and the bands at 2927.04, 2857.97 and 1337.25 cm^{-1} are assigned to ν (C-H of $-\text{CH}_3$ and $-\text{CH}_2-$) absorption, and the band at 1670.40 is assigned to ν (C=O of -HCO) absorption, and the bands at 1619.99, 1580.31, 1542.52 cm^{-1} are assigned to ν (-C=N- and -C=C-) absorption in aromatic ring, and the bands at 649.89, 530.04 cm^{-1} are assigned to ν (Cu-N and Cu-O) absorption. The crystal productivity is 40.79% , based on metal copper ion.

X-ray crystallography

For Cu-1: A blue single crystal of dimension 0.58 \times 0.30 \times 0.23 mm was selected for the measurement . The data of Cu-1 were collected on a Bruke Breeze CCD detector equipped with graphite-monochromatized Mo-K α radiation ($\lambda = 0.71073 \text{ \AA}$) at 296(2)K and used an omega-scan mode in the range of $2.29^\circ \leq \theta \leq 25.10^\circ$ ($-36 \leq h \leq 32$, $-8 \leq k \leq 8$, $-9 \leq l \leq 10$). Computing data collection: Bruker SMART(Bruker, 1998)⁴; computing cell refinement: Bruker SMART(Bruker, 1998); computing data reduction: Bruker SAINT(Bruker, 1998)⁴; computing structure solution and refinement: SHELXL97 (Sheldrick, 2008)⁵; computing molecular graphics: SHELXTL (Sheldrick, 2008). The structure was solved by direct methods using SHELXL-97 and refined by full matrix least- squares on F^2 using the SHELXL 97 program. The non-hydrogen atoms were assigned by anisotropic displacement parameters in the refinement. All H atoms were geometrically positioned and refined using a rotating model for methyl and using a riding model for other groups, with C-H = 0.9300 \AA for aryl [$U_{\text{iso}}(\text{H}) = 1.2 U_{\text{eq}}(\text{C})$], C-H = 0.9700 ~ 0.9800 \AA for secondary and ternary methylene [$U_{\text{iso}}(\text{H}) = 1.2 U_{\text{eq}}(\text{C})$], C-H = 0.9600 \AA for methyl [$U_{\text{iso}}(\text{H}) = 1.5 U_{\text{eq}}(\text{C})$], N-H = 0.8600 ~ 0.9000 \AA for amidogen [$U_{\text{iso}}(\text{H}) = 1.2 U_{\text{eq}}(\text{N})$], and O-H = 0.8200 ~ 0.9253 \AA for water [$U_{\text{iso}}(\text{H}) = 1.5 U_{\text{eq}}(\text{O})$]. The crystal data were given in Table S1, and selected bond lengths and bond angles were listed in Table S2, and hydrogen bond lengths and hydrogen bond angles were listed in Table S3. The molecular structure of Cu-1 with the atom numbering scheme was illustrated in Fig. S2(a,c), and hydrogen-bonded tetramer formed by hydrogen-bondings was illustrated in Fig. S2(b), and 2-D sheet structure of Cu-1 in ac plane was illustrated in Fig. S2(d). The atomic coordinates and other parameters of the structure of Cu-1 had been deposited in the Cambridge Crystallographic Data Center(no. 919835; deposit@ccdc.cam.ac.uk). Copies of the data can be obtained free of charge on application to CCDC, 12 Union Road, CAMBRIDGE CB2 1EZ, UK ; Email:deposit@ccdc.cam.ac.uk.

For Cu-2: A green single crystal of dimension 0.47 \times 0.26 \times 0.20 mm was selected for the measurement . The data of Cu-2 were collected on a Bruke Breeze CCD detector equipped with graphite-monochromatized Mo-K α

radiation ($\lambda = 0.71073 \text{ \AA}$) at 296(2) K and used a phi and omega scans mode in the range of $2.88^\circ \leq \theta \leq 25.10^\circ$ ($-8 \leq h \leq 8$, $-35 \leq k \leq 34$, $-9 \leq l \leq 10$). Computing data collection: Bruker SMART(Bruker, 1998)⁴, computing cell refinement: Bruker SMART(Bruker, 1998); computing data reduction: Bruker SAINT(Bruker, 1998)⁴, computing structure solution and refinement: SHELXL97 (Sheldrick, 2008)⁵ and Olex2 1.2⁶, computing molecular graphics: SHELXTL (Sheldrick, 2008). The structure was solved by direct methods using SHELXL-97 and refined by full matrix least-squares on F^2 using the SHELXL 97 and Olex2 1.2 program. The non-hydrogen atoms were assigned by anisotropic displacement parameters in the refinement. All H atoms were geometrically positioned and refined using a rotating model for water and methyl and using a riding model for other groups, with C–H = 0.9300 Å for aryl [$U_{\text{iso}}(\text{H}) = 1.2 U_{\text{eq}}(\text{C})$], C–H = 0.9700 Å for secondary methylene [$U_{\text{iso}}(\text{H}) = 1.2 U_{\text{eq}}(\text{C})$], C–H = 0.9600 Å for methyl [$U_{\text{iso}}(\text{H}) = 1.5 U_{\text{eq}}(\text{C})$], and O–H = 0.8500 ~ 0.8501 Å for water and O–H = 0.8433 Å for methanol [$U_{\text{iso}}(\text{H}) = 1.5 U_{\text{eq}}(\text{O})$]. Moreover, C(12) and C(13) atomic coordinates and isotropic or equivalent isotropic displacement parameters were refined by restraints and constraints with sigma of 0.01 and sigma for terminal atoms of 0.02. The crystal data were given in Table S1, and selected bond lengths and bond angles were listed in Table S2, and hydrogen bond lengths and hydrogen bond angles were listed in Table S3. The molecular structure of Cu-2 with the atom numbering scheme was illustrated in Fig. S3(a,b), and the 2-D sheet structure containing segregated water-O mixed chains was illustrated in Fig. S3(c), and a water-O mixed chain was illustrated in Fig. S3(d). The atomic coordinates and other parameters of the structure of Cu-2 had been deposited in the Cambridge Crystallographic Data Center(no. 919836; deposit@ccdc.cam.ac.uk). Copies of the data can be obtained free of charge on application to CCDC, 12 Union Road, CAMBRIDGE CB2 1EZ, UK ; Email:deposit@ccdc.cam.ac.uk.

Crystal structure description

For Cu-1: Single-crystal structure analysis reveals that Cu-1 is a chiral binuclear copper (II) coordination compound in orthorhombic crystal system with space group $P2(1)2(1)2$ and flack parameter 0.03(2) (Table S1), and each coordinated unit consists of one Cu(II) cation, half of 4,4'-Bipyridine molecule, one water molecule, one N-(2)-L-alanyl-L-glutamine ligand anion and four crystal water molecules, and the linking 4,4'-bipyridine molecule lies a twofold axis [Fig. S2(a)]. In the structure of Cu-1, the central Cu(II) cation is five coordinated with two N atoms and one O atom of the ligand N-(2)-L-alanyl-L-glutamine anion, one N atom of 4,4'-Bipyridine and one O atom of the water molecule to form a slightly distorted square pyramidal arrangement. The sum of bond angles [$N(1)Cu(1)N(2) = 100.2(2)^\circ$, $N(3)Cu(1)N(2) = 83.07(19)^\circ$, $N(3)Cu(1)O(2) = 82.74(19)^\circ$ and $O(2)Cu(1)N(1) = 92.0(2)^\circ$] is 358.01° , near 360° (Table S2), meaning that Cu(1), N(1), N(2), N(3), and O(2) are almost coplanar. The mean deviation from plane [Cu(1) N(1) N(2) N(3) O(2)] is 0.0592 Å, and the maximum deviation of Cu(1) atom is -0.1480 Å ($25.690x + 3.752y - 1.761z = 11.4788$). The atom O(1) of water molecule is at the apical position in the square pyramidal arrangement with a normal bond length 2.365(5) Å [Cu(1)-O(1)]. The bond length Cu(1)-N(3) [1.929(5) Å, Table S2] is shorter than those of other Cu-O or Cu-N [1.982(5) ~ 2.365(5) Å], indicating that the stronger coordinated ability exists between Cu(II) cation and N atom of dipeptide bond in the N-(2)-L-alanyl-L-glutamine anion. There are many different hydrogen bondings in the structure of Cu-1, which is the characteristic of this structure. It is the hydrogen bond interactions that make four crystal water molecules be linked together to form a hydrogen-bonded tetramer [$O(1w) \cdots O(2w) = 2.907(7) \text{ \AA}$, $O(4w) \cdots O(2w) = 2.929(8) \text{ \AA}$, $O(4w) \cdots O(3w) = 2.994(10) \text{ \AA}$] [Fig. S2(b)], which is anchored by amino, carboxylic and amide groups via different hydrogen-bonding interactions [$N(2) \cdots O(2w) = 3.067(8) \text{ \AA}$; $N(2) \cdots O(3w)^{\#a} = 3.138(8) \text{ \AA}$; $O(3w) \cdots O(3)^{\#f} = 2.771(7) \text{ \AA}$; $N(4) \cdots O(1w)^{\#c} = 2.881(7) \text{ \AA}$; $O(1w) \cdots O(5)^{\#e} = 2.9349(7) \text{ \AA}$; Symmetry codes: (a) $-x+1, -y+1, z$; (c) $x, y, z+1$; (e) $x, y-1, z-1$; (f) $-x+1, -y+1, z-1$]. It is also the hydrogen bond interactions that make the binuclear compound and the water molecules form a pear-shaped structure, and the 4,4'-bipyridine molecule is located in the center of the "pear". These "pears" are ranked orderly in ac plane, and a two-dimensional network structure is formed by

hydrogen bonds [N(4)···O(4)^{#b} = 3.060(8) Å (Symmetry codes: -x+1/2, y-1/2, -z+2); O(3W)···O(3)^{#f} = 2.771(7); N(2)···O(3w)^{#a} = 3.138(8) Å; N(4)···O(1w)^{#c} = 2.881(7) Å] [Table S3; Fig. S2(d)].

For Cu-2: Single-crystal structure analysis reveals that Cu-2 is a centrosymmetric binuclear copper (II) coordination compound in monoclinic crystal system with space group P2(1)/c (Table S1), and each copper (II) coordinated unit consists of one Cu(II) cation, half of 4,4'-Bipyridine molecule, one methanol molecule, one β -[(3-formyl-5-methyl-2-hydroxy-benzylidene)-amino]propionic acid anion [(SB)²⁻] and one crystal water molecules, and 4,4'-Bipyridine molecule acts as a bridge role to link the two coordinated units, and an inversion centre is located in it [Fig. S3(a,b)]. In the structure of Cu-2, the central Cu(II) cation is five coordinated with two O atoms and one N atom of the ligand (SB)²⁻ anion, one N atom of 4,4'-Bipyridine and one O atom of the methanol molecule to form a slightly distorted square pyramidal arrangement. The sum of bond angles [O(3)Cu(1)N(1) = 91.98(12)°, O(3)Cu(1)N(2) = 88.09(12)°, N(1)Cu(1)O(1) = 92.02(12)° and O(1)Cu(1)N(2) = 87.22(12)°] is 359.31°, near to 360° (Table S2), meaning that Cu(1), O(1), N(1), O(3) and N(2) are coplanar. The mean deviation from plane [Cu(1)O(1)N(1)O(3)N(2)] is 0.0721 Å, and the maximum deviation of Cu(1) atom is -0.1008 Å [3.281 x - 2.545 y + 6.975z = 0.7969]. The O(5) atom of methanol molecule is at apical position in the square pyramidal arrangement. The bond lengths (1.910 ~ 2.330 Å) of Cu-N or Cu-O are in the normal range (Table S2). The O atoms [O(2)] of carbonyl of carboxyl in ligand (SB)²⁻ anions (one of two Schiff base bonds was broken during the process of synthesis of Cu-2.) act as the roles of hydrogen bond acceptors, and the crystal water molecules O(1W) act as the roles of hydrogen bond donors. A "z" shaped water-O mixed chain is formed via the hydrogen bonds [O(1W)···O(2)^{#a} = 2.872(4) Å and O(1W)···O(2)^{#b} = 2.921(5) Å, symmetry codes: (a) x-1, y, z+1; (b) x-1, -y+3/2, z+1/2] between the O(2) atoms and water molecules O(1W) [Table S3, Fig. S3(d)]. Moreover, the O(5) atoms of methanol molecules are linked by water molecules O(1W) via hydrogen bonds [O(5)···O(1W)^{#c}, symmetry code: (a) x, y, z-1] to further form a two-dimensional network structure in bc plane [Fig. S3(c)].

Cell viability assay

Cell viability was determined by measuring the ability of cells to transform MTT (3-(4,5-Dimethyl-2-Thiazolyl)-2,5-diphenyltetrazolium bromide) to a purple formazan dye. Cells were grown in a DMEM medium supplemented with FBS (10%), penicillin (100 $\mu\text{g}\cdot\text{mL}^{-1}$), and streptomycin (100 $\mu\text{g}\cdot\text{mL}^{-1}$). They were incubated at 37°C in a humidified incubator with 5% CO₂ and 95% air. Cells at the exponential growth phase were diluted to 6 × 10⁴ cells per mL with DMEM, and were seeded in 96-well plates at a volume of 100 μL per well with six duplicates. The other empty wells were filled with 1 × PBS. Cells were incubated at 37°C in 5% CO₂ for 24 h, and were treated with various concentrations of complex (100 μL per well) diluted with DMEM medium without FBS. The medium and drug-free control samples were prepared simultaneously. After incubation of the cells for up to 48 h, MTT (20 μL , 5 mg mL⁻¹) solution was added to each well. After a further period of incubation (4 h at 37°C in 5% CO₂), DMSO (150 μL) was added to each well. The plates were oscillated for 10 minutes, and the values of OD were analyzed by an ELX800 type Microplate Reader (Bio-Tek, USA) at a wavelength of 570 nm. The percentage growth inhibitory rate of treated cells was calculated by $(\text{OD}_{\text{tested}} - \text{OD}_{\text{media control}}) / (\text{OD}_{\text{drug-free control}} - \text{OD}_{\text{media control}}) \times 100\%$, where OD is the mean value calculated by using the data from six replicate tests. The IC₅₀ values were determined by plotting the percentage viability versus concentration on a logarithmic graph and by reading the concentration at which 50% of cells were viable, relative to the control.

Apoptosis assay

Apoptosis was detected with an Annexin V/PI kit purchased from BD Pharmingen (BD Bioscience) according to the manufacturer's instructions. HUVECs or HeLa cells were seeded in 6-well plates, and were allowed to grow

into 60-70% confluence, and were treated with Cu-1 (40 μM) or Cu-2 (1.25, 2.5 and 5 μM) for 48h. To detect early and late apoptosis, both floating and adherent cells were harvested together and washed twice with $1\times\text{PBS}$, and were centrifuged at $1000\text{ r}\cdot\text{min}^{-1}$ for 5 min to remove the medium, and were resuspended in Binding Buffer $200\mu\text{L}$ at a concentration of 10^6 cells per mL. Subsequently, 10 μL of Annexin V-FITC were added to the above Binding Buffer to stain cells. Cells were incubated for 10 min at 37°C in the dark, and were centrifuged at $1000\text{ r}\cdot\text{min}^{-1}$ for 5 min to remove the Binding Buffer, and were resuspended in Binding Buffer $200\mu\text{L}$ again. 10 μL of PI (propidium iodide) were added to the Binding Buffer to stain cells, and cells were analyzed by a FACS Calibur (BD Bioscience).

HUVECs migration assay

HUVECs were allowed to grow into full confluence in 6-well plates precoated with 0.1% gelatin and then incubated with $10\mu\text{g}\cdot\text{mL}^{-1}$ of mitomycin C at 37°C , 5% CO_2 for 12 h to inactivate HUVECs. Monolayer inactivated HUVECs were wounded by scratching with a $200\mu\text{L}$ pipette tip. Fresh endothelial cell growth medium (ECGM) was added with different concentrations of complexes in presence or absence vascular endothelial growth factor (VEGF) stimulation. After 24 h of incubation at 37°C , 5% CO_2 , images were taken by an inverted photomicroscope with the same magnification. The distances that cells migrated were quantified by manual measurement, and percentage inhibition was expressed using untreated wells at 100%. At least three independent experiments were performed.

Tube formation assay

Matrigel was dissolved at 4°C for overnight according to the product description, and each well of prechilled 96-well plates was coated with $60\mu\text{L}$ matrigel and then incubated at 37°C for 20 minutes. HUVECs (2.5×10^4 cells) were seeded into each well with $200\mu\text{L}$ endothelial cell growth medium with various concentration of complexes in presence or absence VEGF stimulation. After 24 h of incubation at 37°C , 5% CO_2 , endothelial cell tube formations were assessed with an inverted photomicroscope. Tubular structures were quantified by manual counting of low-power fields and percentages of tube-like structure formations were expressed using untreated wells as 100%.

Chicken chorioallantoic membrane (CAM) assay

The CAM is used as a model system for chemically inducing and suppressing tumor angiogenesis assays. Fertilized chicken eggs (10 eggs per group) were incubated at 37°C and 80% humidity. On the sixth day of incubation, a square window was opened in the shell, and CAMs were injected with different test compounds by insulin syringe. The window was sealed with a transport tape after injection, and eggs were returned to the incubator. After 4 days of incubation, CAM arterious branches in each treatment group were photographed and counted by using a Nikon digital camera system (Chiyoda-ku, Tokyo, Japan). The anti-angiogenic effect of the test compounds was presented as relative number of arterious branches.

Cell uptake and uptake mechanism assay

Cell uptake assay

HUVECs or HeLa cells were seeded in 6-well plates (2×10^5 cells per well) on the day before treatment. The medium was replaced, and cells were exposed to Cu-2 (5 μM) for 24 h. Both floating and adherent cells were harvested together, and were washed twice with $1\times\text{PBS}$, and were centrifuged at $1000\text{ r}\cdot\text{min}^{-1}$ for 5 min to remove the PBS, and were resuspended in PBS $1000\mu\text{L}$ at a concentration of 10^6 cells per mL. Subsequently, the

fluorescence strengths of Cu-2 were analysed using flow cytometry with excitation wavelength 444.0 nm and emission wavelength 517.4 nm.

uptake mechanism assay by confocal microscopy

HUVECs or HeLa cells were seeded into chambers (14 mm) for confocal microscopy (1×10^4 cells per chamber), and were allowed to grow into 70~80% confluence. Energy-dependent pathway: Cells were cooled at 4°C for 30 minutes and then were incubated with 5 μ M Cu-2 (10% PBS: 90% serum-free media) at 4°C for 1 hour. Cells were washed thrice with $1 \times$ PBS, and were imaged by confocal microscopy. Non-endocytotic mechanism of uptake: Endocytosis is known as a general entry mechanism, and is an energy-dependent uptake route. We used the endocytic inhibitors colchicine and ammonium chloride to assess the contribution of the endocytotic pathway for Cu-2 uptake and entrance into the nuclei of cells. When cells grew into 70~80% confluence, the medium was replaced in serum-free conditions throughout. The cells were preincubated with colchicine (0.1, 1, 10 μ M) or ammonium chloride (5, 20, 50 μ M) for 1 h at 37°C, and then were co-incubated with 5 μ M Cu-2 at 37°C for 1h. subsequently, cells were washed thrice with $1 \times$ PBS, and were imaged by confocal microscopy with excitation wavelength 444.0 nm and emission wavelength 517.4 nm.

uptake mechanism assay by flow cytometry

HUVECs or HeLa cells were seeded into 6-well plates (2×10^5 cells per well) and were allowed to grow into 90% confluence. The medium was replaced in serum-free conditions throughout. Cells were exposed to Cu-2 (5 μ M) under the same conditions as confocal microscopy images including energy-dependent and non-endocytotic uptake. Subsequently, both floating and adherent cells were harvested together and were washed twice with $1 \times$ PBS. Cells were centrifuged at 1000 r.min⁻¹ for 5 min to remove the PBS, and were resuspended in PBS 1000 μ L at a concentration of 10^6 cells per mL. The fluorescence strengths of Cu-2 were analysed using flow cytometry with excitation wavelength 444.0 nm and emission wavelength 517.4 nm.

Western blot assay

Anti-Akt, Anti-phospho-Akt (Ser473), Anti-Erk1/2, and Anti-phospho-Erk1/2 (Thr202/Tyr204) were obtained from Cell Signaling Technology (Beverly, MA). Anti-GAPDH was obtained from Kangchen (Shanghai, China). Goat anti-mouse IgG and Goat anti-rabbit IgG were obtained from Calbiotech (San Diego, CA).

HUVECs or HeLa cells were seeded into the 100 mm plate (7.5×10^5 cells per plate) on the day before treatment, respectively. The medium was replaced, and cells were exposed to the corresponding compounds for 36 h. The whole-cell lysates were collected, and were boiled for 10 min in $1 \times$ SDS loading buffer, and sequentially were subjected to 5% and 10% SDS-PAGE, and were transferred to nitrocellulose (Amersham Life Sciences). The blots were blocked in blocking buffer (5% nonfat drymilk / 1% Tween-20 in TBS) for 2 h at room temperature and then were incubated with primary antibodies (anti-GAPDH, anti-phospho-Erk1/2, anti-Akt and anti-phospho-Akt, 1:1000) in blocking buffer for 2 h at room temperature. The bands were then visualized using horseradish peroxidase-conjugated secondary antibodies (1:1000) followed by ECL (Pierce Biotech, Rockford, IL). Stripping buffer was used in the western blot assay.

Measurement of intracellular ROS

ROS assay by flow cytometry

HUVECs or HeLa cells were seeded into 6-well plates (2×10^5 cells per well) on the day before treatment. The medium was replaced, and cells were exposed to the corresponding compounds and vitamin C with various concentrations for 24 h or with a fixed concentration for 6h, 12h and 24h. Cells were harvested, and were washed twice with $1 \times$ PBS, and were centrifuged at 1000 r.min^{-1} for 5 min to remove the PBS, and were suspended in PBS ($1 \times 10^6 \text{ cells mL}^{-1}$) with DCFH-DA (10 mM), and were incubated at $37 \text{ }^\circ\text{C}$ for 15 min. Then cells were washed thrice with $1 \times$ PBS to remove extracellular fluorescent agent, and cells were suspended in $1 \times$ PBS solution (500 μL) again, and then the fluorescence intensity of DCF was analysed by flow cytometry.

ROS assay by confocal microscopy

HUVECs or HeLa cells were seeded into the chambers (14 mm) for confocal microscopy (1×10^4 cells per chamber), and were allowed to grow into 60~70% confluence. Cells were exposed to the corresponding compounds and vitamin C with various concentrations for 24 h. After removing the medium, cells were washed twice with $1 \times$ PBS, and were stained in PBS with DCFH-DA (10 mM) at $37 \text{ }^\circ\text{C}$ for 15 min. The fluorescence intensity of DCF was analysed by confocal microscopy.

Supplementary Table

Table S1. Crystal data and structure refinement parameters for complexes Cu-1 and Cu-2.

Parameters	Cu-1	Cu-2
Empirical formula	$[\text{Cu}_2(\text{C}_{10}\text{H}_8\text{N}_2)(\text{C}_8\text{H}_{13}\text{N}_3\text{O}_4)_2(\text{H}_2\text{O})_2] \cdot 8\text{H}_2\text{O}$	$[\text{Cu}_2(\text{C}_{10}\text{H}_8\text{N}_2)(\text{C}_{12}\text{H}_{11}\text{NO}_4)_2(\text{CH}_3\text{OH})_2] \cdot 2\text{H}_2\text{O}$
Formula weight	893.87	849.82
Temperature (K)	296(2)	293(2)

Wavelength (Å)	0.71073	0.71073
Crystal system, space group	Orthorhombic, P2(1)2(1)2	Monoclinic, P2(1)/c
Unit cell dimensions(Å, °)		
<i>a</i>	30.60(6)	7.3882(5)
<i>b</i>	7.415(14)	29.4687(19)
<i>c</i>	8.890(16)	8.6809(6)
β	90.00	99.775(7)
V (Å ³)	2017(7)	1862.6(2)
Z, D _{Calcd} (Mg.m ⁻³)	2, 1.471	2, 1.515
Absorption coefficient (mm ⁻¹)	1.134	1.210
F(000)	936	880
Crystal size (mm ³)	0.58 × 0.30 × 0.23	0.47 × 0.26 × 0.20
θ range for data collection	2.29 25.10	2.88 25.10
Limiting indices	-36 ≤ h ≤ 32 -8 ≤ h ≤ 8 -9 ≤ h ≤ 10	-8 ≤ h ≤ 8 -35 ≤ h ≤ 34 -9 ≤ h ≤ 10
Reflections collected	10933	7883
Independent reflections	3586(<i>R</i> _{int} = <u>0.097</u>)	3315(<i>R</i> _{int} = <u>0.032</u>)
Observed data	2264 (<i>I</i> > 2σ(<i>I</i>))	2585 [<i>I</i> > 2σ(<i>I</i>)]
Refinement method	Full-matrix least-squares on <i>F</i> ²	Full-matrix least-squares on <i>F</i> ²
Nref/Npar/Nres	3586/245/0	3315/248/12
Final <i>R</i> , <i>wR</i> , <i>S</i> [<i>I</i> > 2σ(<i>I</i>)]	<i>R</i> = 0.0474, <i>wR</i> = 0.0785, <i>S</i> = 0.936 <i>w</i> = 1/[σ ² (<i>F</i> _o ²) + (0.0002 <i>P</i>) ² + 0.0000 <i>P</i>] where <i>P</i> = (<i>F</i> _o ² + 2 <i>F</i> _c ²)/3	<i>R</i> = 0.0493, <i>wR</i> = 0.1061, <i>S</i> = 1.059 <i>w</i> = 1/[σ ² (<i>F</i> _o ²) + (0.0420 <i>P</i>) ² + 2.4171 <i>P</i>] where <i>P</i> = (<i>F</i> _o ² + 2 <i>F</i> _c ²)/3
Final <i>R</i> , <i>wR</i> , <i>S</i> (all data)	<i>R</i> = 0.0600, <i>wR</i> = 0.0804, <i>S</i> = 0.936	<i>R</i> = 0.0685, <i>wR</i> = 0.1146, <i>S</i> = 1.132
Shift max / mean	0.000 / 0.000	0.002 / 0.000
Flack parameter *	0.03(2)	
CCDC	919835	919836

* Flack H D (1983), Acta Cryst. A39, 876-881.

Table S2. Selected bond distances (Å) and angles (°) for complexes Cu-1 and Cu-2.

complex Cu-1					
Bond	Dist. (Å)	Bond	Dist. (Å)	Bond	Dist. (Å)
Cu(1)—N(1)	2.025 (5)	Cu(1)—N(2)	2.030 (5)	Cu(1)—N(3)	1.925 (5)
Cu(1)—O(2)	1.982 (5)	Cu(1)—O(1)	2.365 (5)	C(8)—O(4)	1.233 (7)
C(10)—O(3)	1.263 (7)	C(10)—O(2)	1.275 (7)	C(13)—O(5)	1.232 (6)
C(13)—N(4)	1.328 (7)	C(1)—N(1)	1.369 (7)	C(3)—C(3) ^{#i}	1.481 (9)
Angle	(°)	Angle	(°)	Angle	(°)
N(1)—Cu(1)—N(2)	100.2 (2)	N(3)—Cu(1)—N(2)	83.07 (19)	N(3)—Cu(1)—O(2)	82.74 (19)
O(2)—Cu(1)—N(1)	92.0 (2)	N(3)—Cu(1)—N(1)	169.90 (17)	O(2)—Cu(1)—N(2)	161.94 (17)
N(3)—Cu(1)—O(1)	102.4 (2)	O(2)—Cu(1)—O(1)	96.29 (16)	N(1)—Cu(1)—O(1)	86.7 (2)
N(2)—Cu(1)—O(1)	97.62 (17)	O(3)—C(10)—O(2)	123.7 (6)	O(3)—C(10)—C(9)	118.3 (7)
O(4)—C(8)—N(3)	127.0 (6)	O(4)—C(8)—C(7)	120.0 (6)	O(5)—C(13)—N(4)	123.2 (5)
complex Cu-2					
Bond	Dist. (Å)	Bond	Dist. (Å)	Bond	Dist. (Å)
Cu(1)—O(3)	1.910 (3)	Cu(1)—N(1)	1.955 (3)	Cu(1)—O(1)	1.960 (3)
Cu(1)—N(2)	2.050 (3)	Cu(1)—O(5)	2.330 (3)	C(11)—O(4)	1.180 (6)
C(1)—O(2)	1.238 (5)	C(1)—O(1)	1.268 (5)	C(16)—N(2)	1.305 (5)
C(12)—N(2)	1.309 (6)	C(14)—C(14) ^{#i}	1.483 (7)	C(4)—N(1)	1.283 (5)
Angle	(°)	Angle	(°)	Angle	(°)
O(3)—Cu(1)—N(1)	91.98 (12)	O(3)—Cu(1)—N(2)	88.09 (12)	N(1)—Cu(1)—O(1)	92.02 (12)
O(1)—Cu(1)—N(2)	87.22 (12)	O(3)—Cu(1)—O(1)	167.86 (14)	N(1)—Cu(1)—N(2)	176.47 (14)
O(3)—Cu(1)—O(5)	94.76 (15)	N(1)—Cu(1)—O(5)	91.67 (13)	O(1)—Cu(1)—O(5)	96.58 (15)
N(2)—Cu(1)—O(5)	91.84 (13)	O(4)—C(11)—C(9)	126.1 (5)	O(2)—C(1)—O(1)	123.1 (4)

Symmetry codes: For complex Cu-1: (i) $-x+1, -y, z$; For complex Cu-2: (i) $-x+2, -y+2, -z$.

Table S3. Hydrogen bond lengths (Å) and angles (°) for complexes Cu-1 and Cu-2.

Cu-1				
<i>D—H···A</i>	<i>D—H</i>	<i>H···A</i>	<i>D···A</i>	<i><DHA</i>
N(2)—H(2A)···O(3W) ^{#a}	0.90	2.25	3.138 (8)	168.6
N(2)—H(2B)···O(2W)	0.90	2.18	3.067 (8)	167.6
O(1)—H(1B)···O(2)	0.83	2.81	3.248 (6)	115.0
N(4)—H(4A)···O(4) ^{#b}	0.86	2.29	3.060(8)	149.7
N(4)—H(4B)···O(1W) ^{#c}	0.86	2.03	2.881 (7)	170.3
O(1)—H(1A)···O(4) ^{#d}	0.82	2.01	2.808(7)	164.0
O(4W)—H(4WA)···O(2W)	0.84	2.53	2.929 (8)	110.8
O(2W)—H(2WA)···O(4) ^{#d}	0.86	1.92	2.788 (7)	177.3
O(1W)—H(1WA)···O(5) ^{#e}	0.85	2.09	2.934 (7)	171.7
O(1W)—H(1WB)···O(2W)	0.85	2.36	2.907 (7)	122.3
O(3W)—H(3WB)···O(3) ^{#f}	0.83	2.33	2.771 (7)	114.2
O(2W)—H(2WB)···O(1W)	0.87	2.36	2.907 (7)	121.1
O(4W)—H(4WB)···O(3W)	0.93	2.27	2.994(10)	134.3

Cu-2				
<i>D—H···A</i>	<i>D—H</i>	<i>H···A</i>	<i>D···A</i>	<i><DHA</i>
O(1W)—H(1WB)···O(2) ^{#a}	0.85	2.06	2.872 (4)	159.8
O(1W)—H(1WA)···O(2) ^{#b}	0.85	2.08	2.921 (5)	167.8
O(5)—H(5B)···O(1W) ^{#c}	0.84	1.91	2.735 (4)	164.4

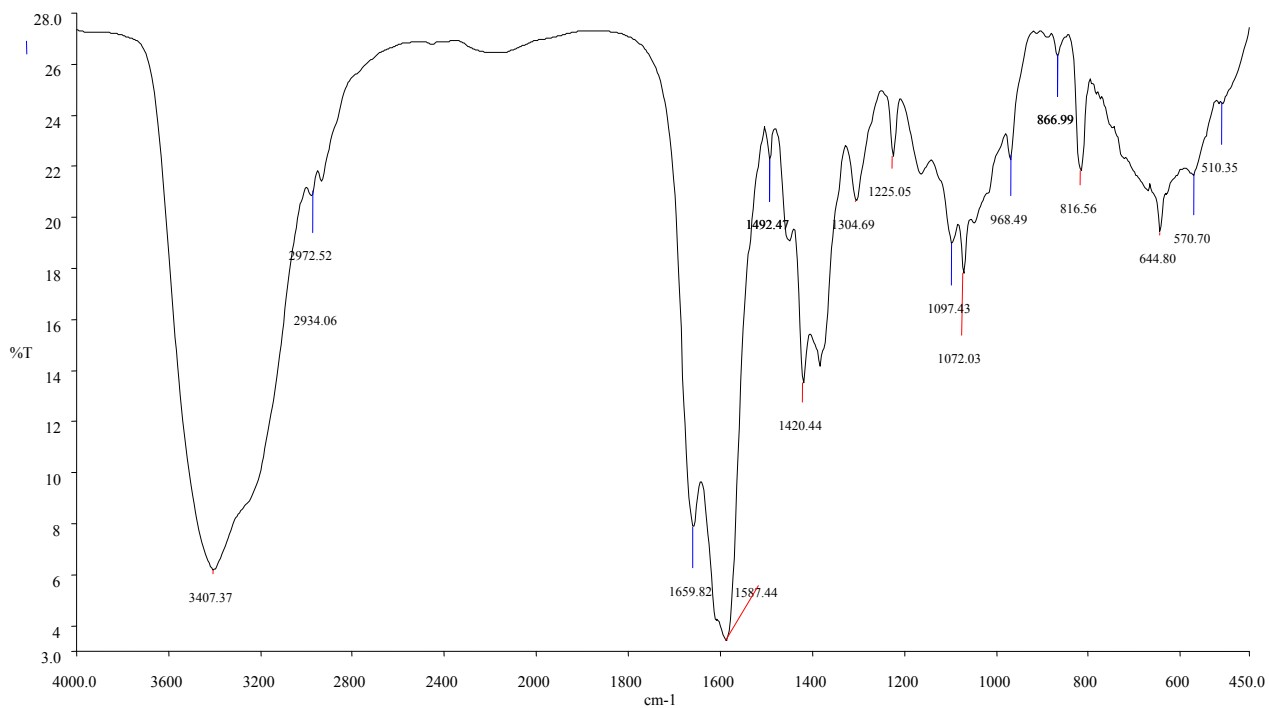
Symmetry codes:

For complex Cu-1: (a) $-x+1, -y+1, z$; (b) $-x+1/2, y-1/2, -z+2$; (c) $x, y, z+1$; (d) $x, y-1, z$; (e) $x, y-1, z-1$;

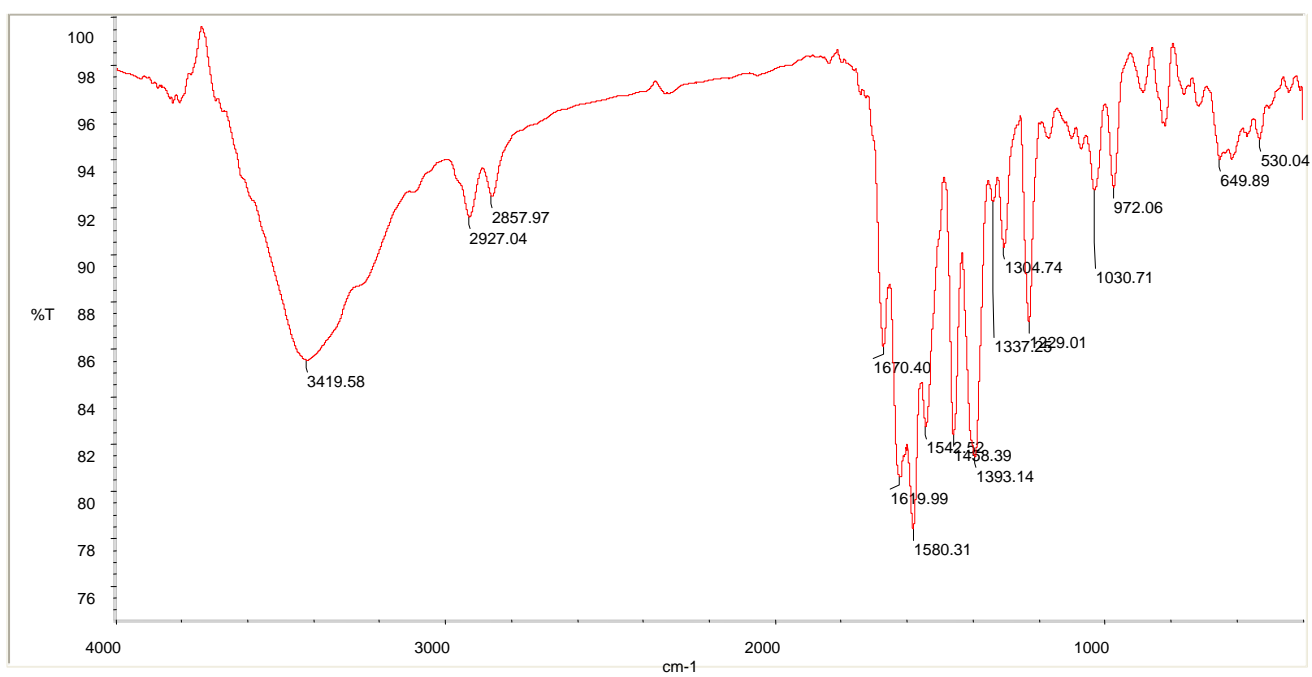
(f) $-x+1, -y+1, z-1$.

For complex Cu-2: (a) $x-1, y, z+1$; (b) $x-1, -y+3/2, z+1/2$; (c) $x, y, z-1$.

Supplementary Figures



(a)



(b)

Fig. S1 IR spectra of Cu-1 (a) or Cu-2 (b) with KBr pallets in the range of 4000~400 cm⁻¹.

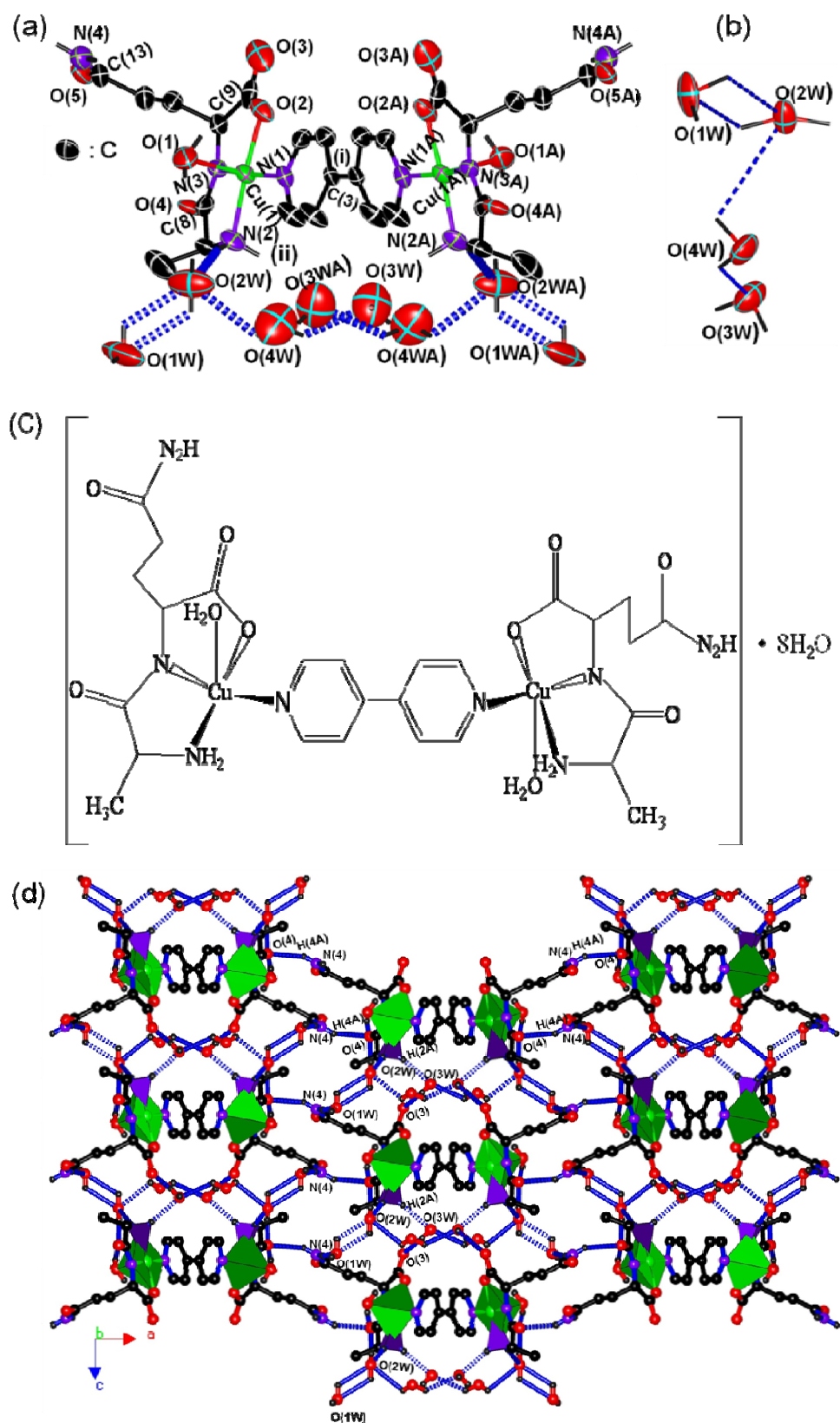


Fig. S2. (a).Molecular view of Cu-1 using atom labelling scheme. Ellipsoids were drawn at the 50% probability level. Symmetry code: (i) $-x+1, -y, z$; (b). Hydrogen-bonded tetramer is formed by hydrogen bonding interactions in the structure of Cu-1. (c) The chemical structure of Cu-1. (d) A view of 2-D sheet structure of Cu-1 in ac plane. Some H atoms were omitted for clarity.

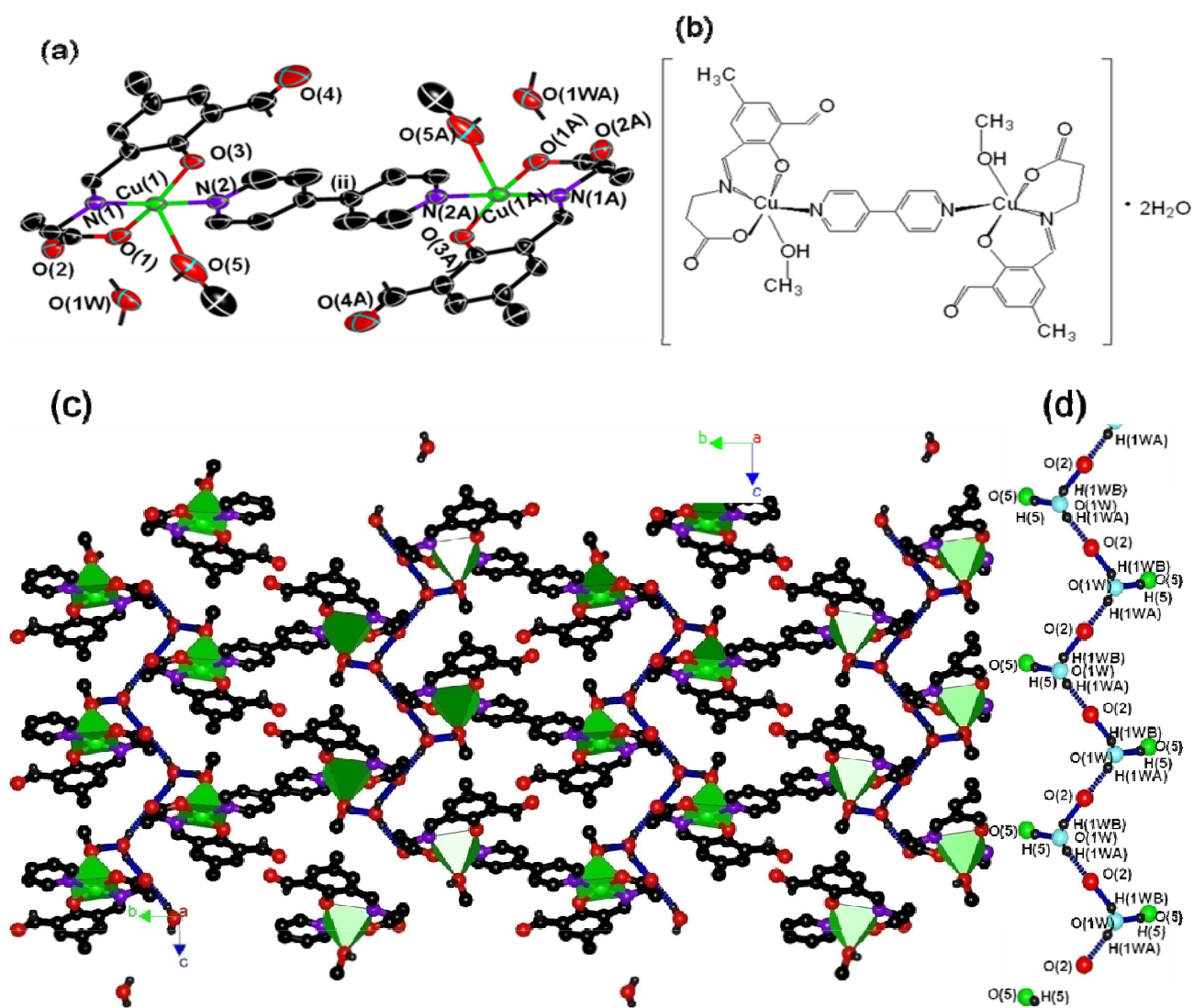


Fig. S3. (a) Molecular view of Cu-2 using atom labelling scheme. Ellipsoids were drawn at the 50% probability level. Symmetry code: (ii) $-x+2, -y+2, -z$; (b) The chemical structure of Cu-2. (c) A view of 2-D sheet structure of Cu-2 in bc plane. Some H atoms were omitted for clarity. (d) Schematic diagram of 1D water-O mixed chain in Cu-2. It is the water-O mixed chains that steady the 2-D sheet structure of Cu-2.

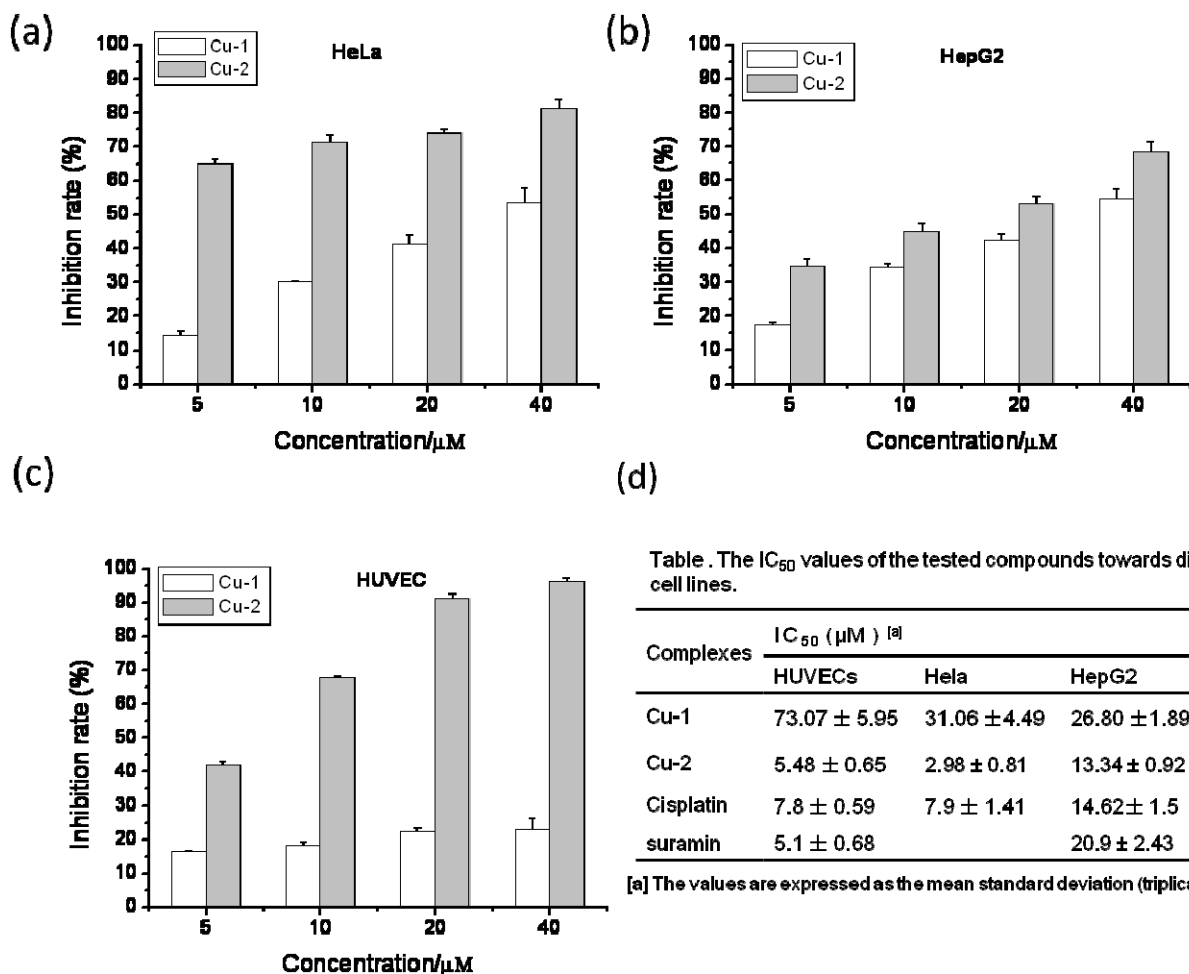


Fig. S4. Compounds inhibit cell viability in HeLa cells, HepG2 cells and HUVECs. Cu-1 and Cu-2 inhibit cells proliferation effects on HeLa (a), HepG2 (b) and HUVEC (c) in the range of 0 ~ 40 μM . Cu-1 and Cu-2 inhibit cell viability in a dose-dependent manner. Cells (6×10^3 per well) were incubated for 24h with 10 % FBS medium and then were treated by different concentrations of Cu-1 or Cu-2 for 48h. Cell viability was quantified by using a MTT method. (d) The table of the values of IC_{50} , and IC_{50} was identified as the compounds concentration to inhibit 50% cell proliferation. Cu-2 exhibited more effective activities than Cu-1 in terms of cell growth inhibition, with a distinct preference for HeLa cells and HUVECs, and Cu-2 inhibited the proliferation of HeLa cells more strongly than HUVECs at a low concentration.

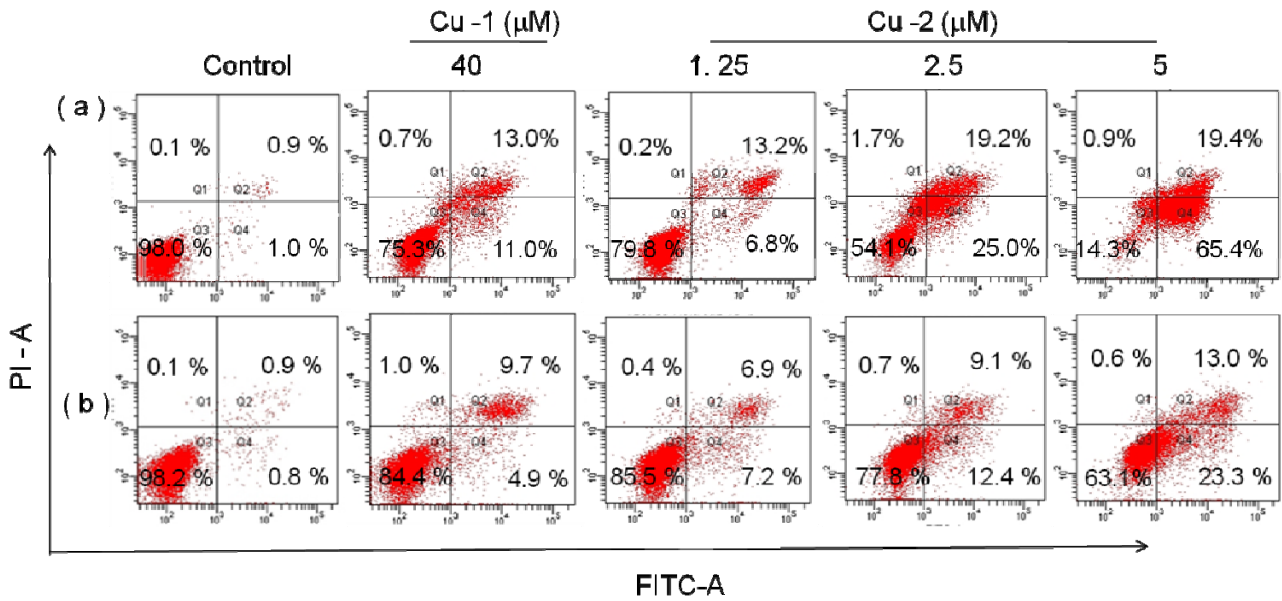


Fig. S5. HeLa cells and HUVECs were double-stained with annexin V/PI and were analysed induced-apoptosis of HeLa cells (a) and HUVECs (b) by flow cytometry after treatment with Cu-1(40μM) or with various concentrations of Cu-2 for 48 h. The experiments were performed in three independent experiments. This figure shows one of the three independent experiments. Cu-2 could significantly induce apoptosis in HeLa cells and HUVECs compared with Cu-1 in a dose-dependent manner.

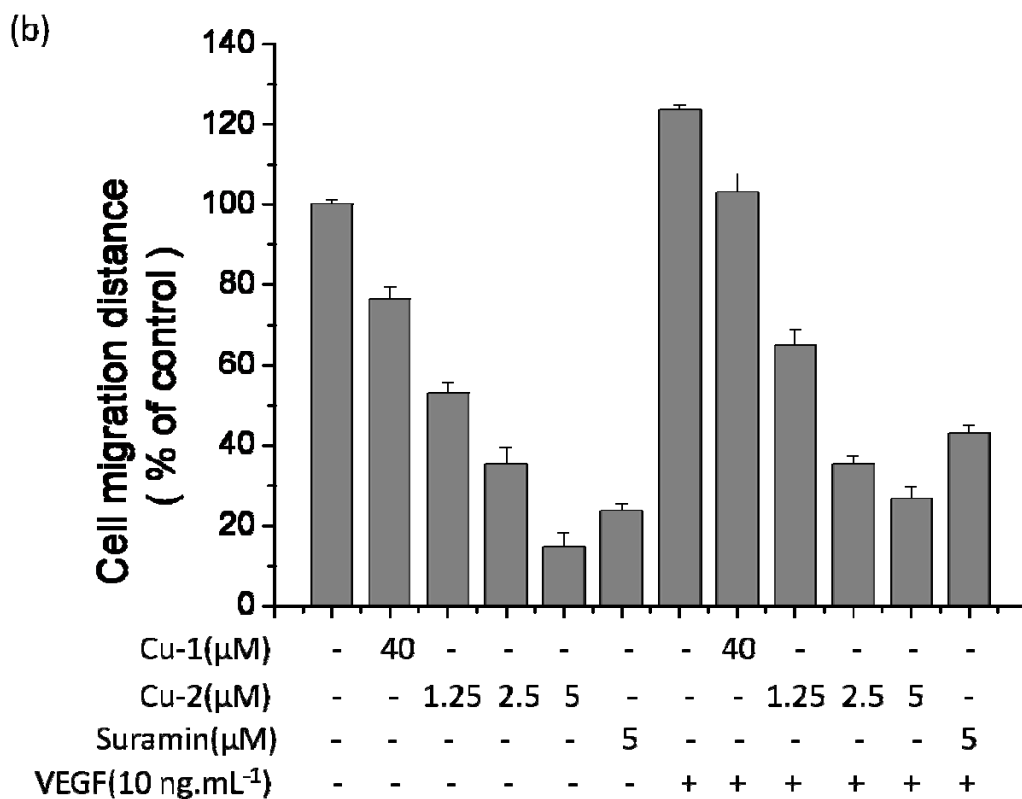
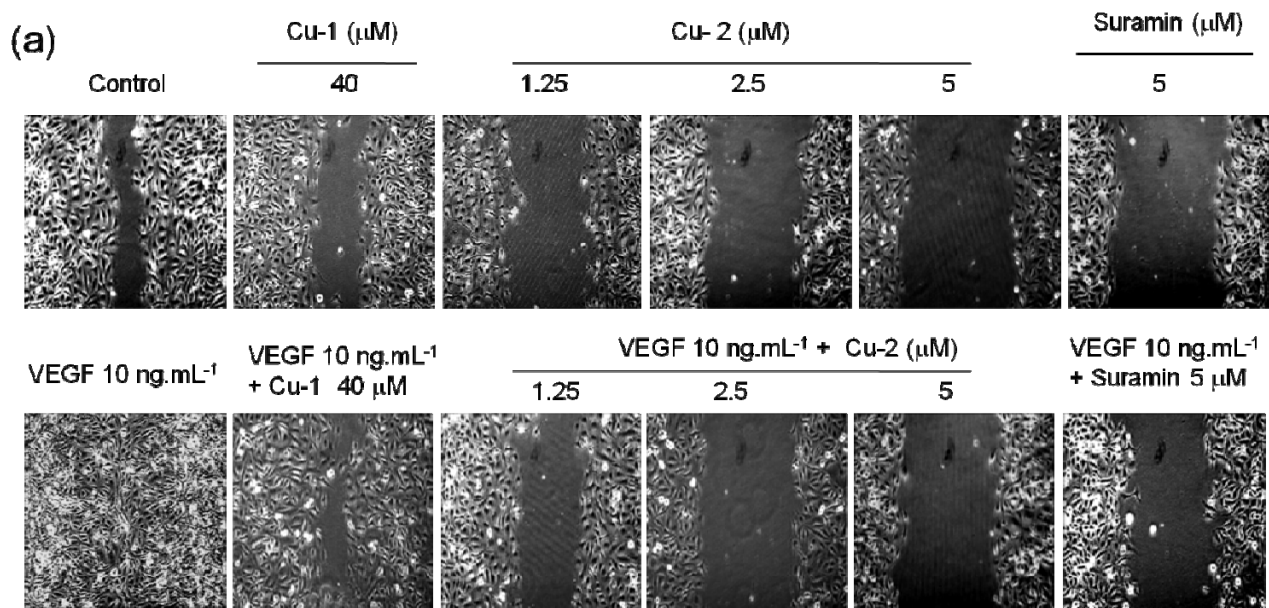


Figure S6 (a) Effects of Cu-1, Cu-2 and suramin on HUVECs migration in wound migration assays in the presence or absence of VEGF stimulation, respectively. Cells were wounded with a pipette tip. After cells were incubated for 24 h, images of HUVEC wound migration were taken with an inverted photomicroscope at 10 × magnification. (b) After incubation, the migrate distances were quantified by manual measurement. These experiments were performed thrice with similar results, and significant differences from control group were observed ($p < 0.05$) Data were presented as the percentages of the control group, which was set at 100%. Cu-2 is more advantageous than Cu-1 and suramin in inhibiting the migrations of inactivated HUVECs in a dose-dependent manner in the presence or absence of VEGF stimulation.

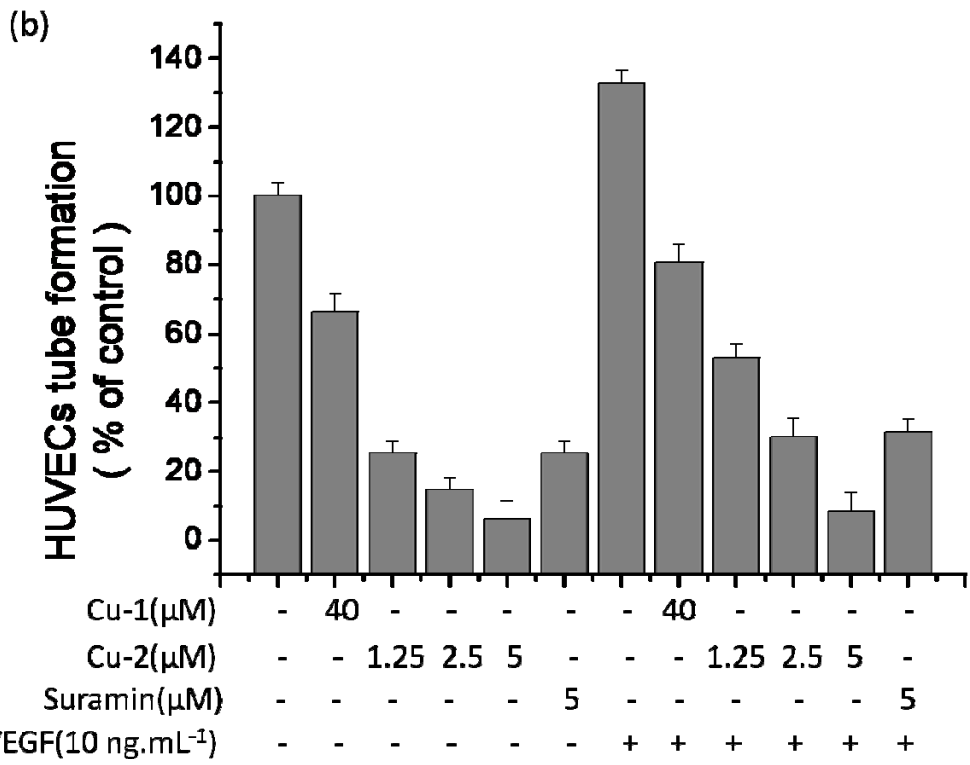
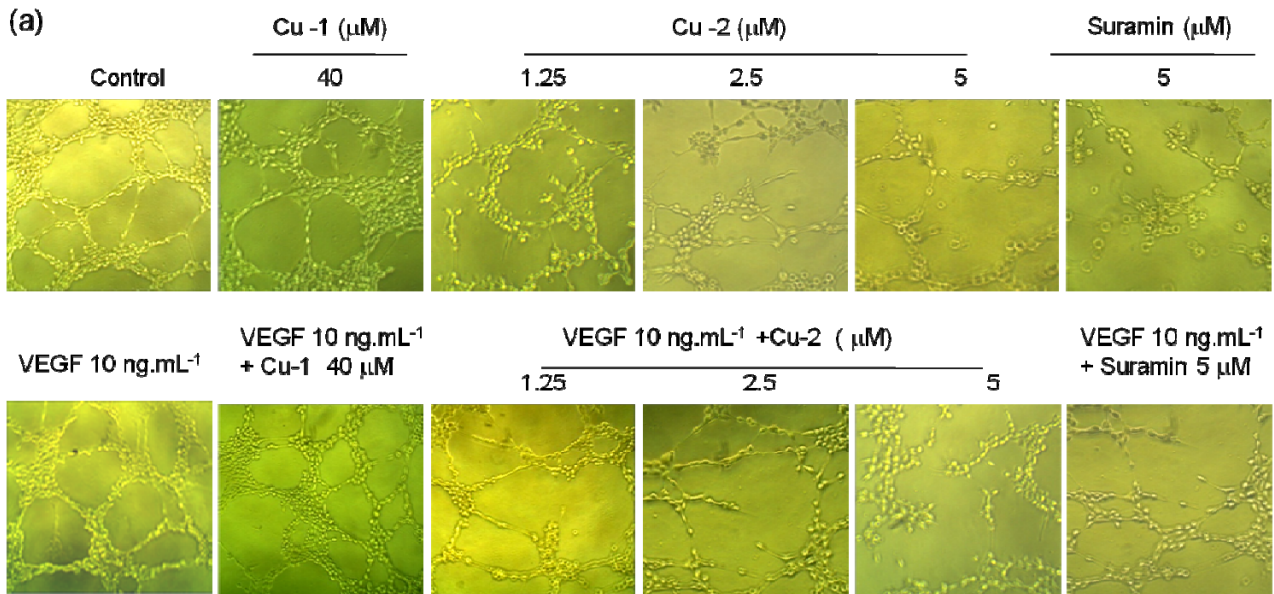


Fig. S7. Effects of Cu-1, Cu-2 and suramin on HUVECs tube formations in the presence or absence of VEGF stimulation. HUVECs (2.5×10^4) were treated with Cu-1, or Cu-2, and or suramin in the presence or absence of VEGF stimulation, and were added on matrigel layers. (a) After cells were incubated for 24 h, images of HUVEC tube-like formations were taken with an inverted photomicroscope at $10 \times$ magnification. (b) The tube-like formations were quantified by manual counting. These experiments were performed thrice with similar results, and significant differences from control group were observed ($p < 0.05$). Data are presented as the percentages of the control group, which was set at 100%. Cu-2 is more advantageous than Cu-1 and suramin in inhibiting tube formations of HUVECs in a dose-dependent manner in the presence or absence stimulation of VEGF stimulation.

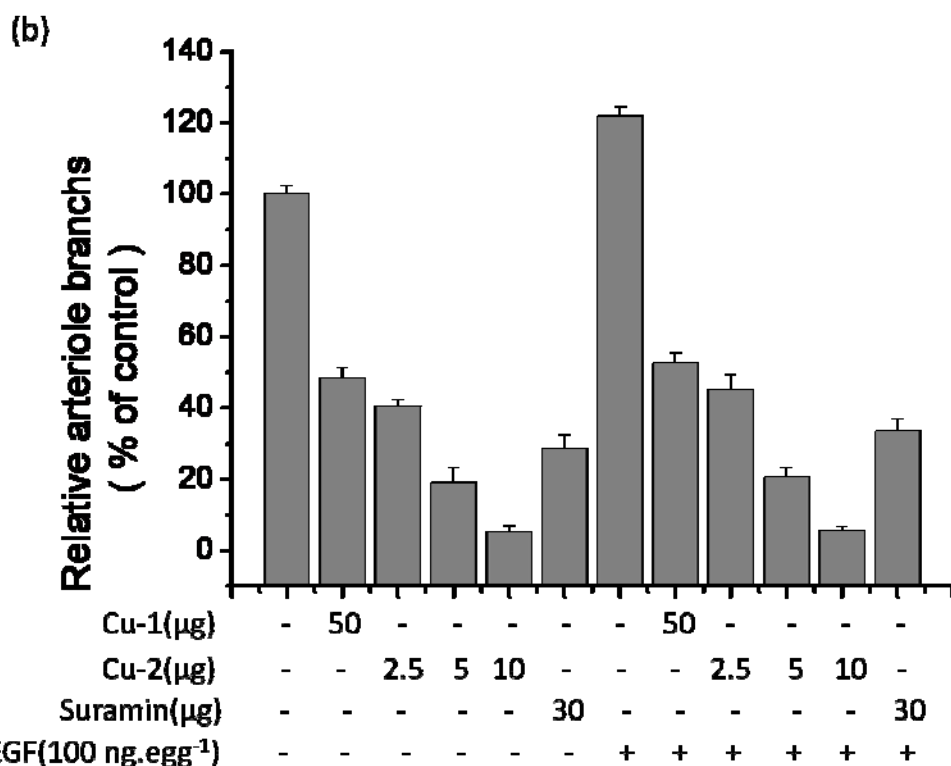
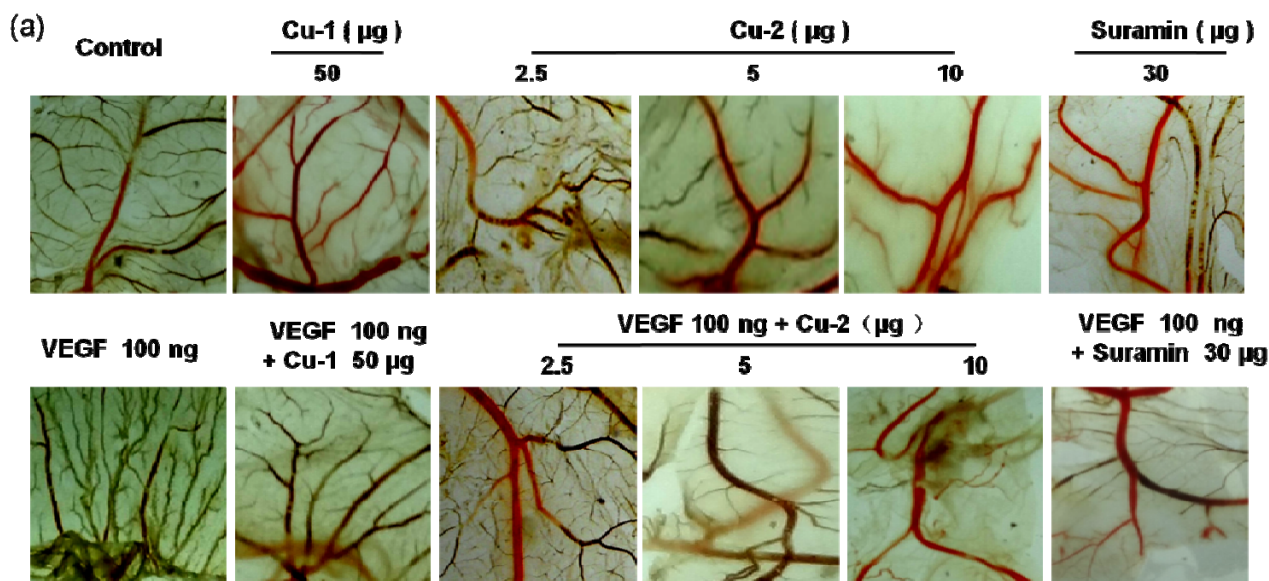


Fig. S8. (a) Angiogenic development of the arterial endpoint in the CAM was stimulated by VEGF and was inhibited by Cu-1 or Cu-2. The chick embryos were treated with PBS (Control), Cu-1, Cu-2; suramin; VEGF; VEGF + Cu-1, VEGF + Cu-2, and VEGF + suramin, respectively. The various test compounds were injected into the CAM of fertilized chicken eggs on day 6 of development, and the anti-angiogenic effects of the test compounds were observed at 4 d after injection. The images were taken with a Nikon digital camera system. (b) The arteriole branches were quantified by manual counting. These experiments were performed thrice with similar results and significant differences from control group were observed ($p < 0.05$). Data were presented as the percentages of the control group, which was set at 100%. Cu-2 is more advantageous than Cu-1 and suramin in blocking chicken CAMs in a dose-dependent manner in the presence or absence of VEGF stimulation.

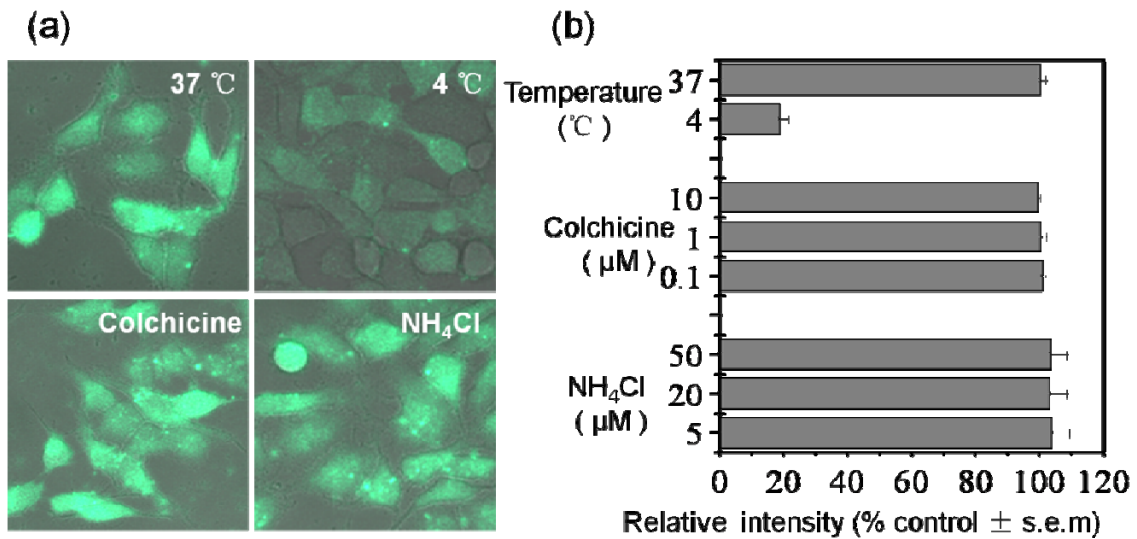


Fig. S9. Cellular uptake mechanisms of Cu-2 (excitation wavelength = 444.0 nm; emission wavelength = 517.4 nm) in HeLa cells (a) Cellular uptake mechanisms were analysed by confocal microscopy after treatment with Cu-2 (5 μM) for 1 h at 4 °C or 37 °C and after treatment with endocytosis inhibitors colchicines or ammonium chloride for 1 h, then co-incubation with Cu-2 (5 μM) for other 1 h in HeLa cells. (b) Cellular uptake mechanisms were analysed by flow cytometry under the same conditions as in confocal microscopy in HeLa cells. Cu-2 uptake increased as temperature increased in HeLa cells, indicating that Cu-2 enters the cells via an energy-dependent pathway. Moreover, these well-studied endocytotic pathways are not responsible for the uptake of Cu-2, indicating that Cu-2 entering the cells are consistent with a non-endocytotic uptake.

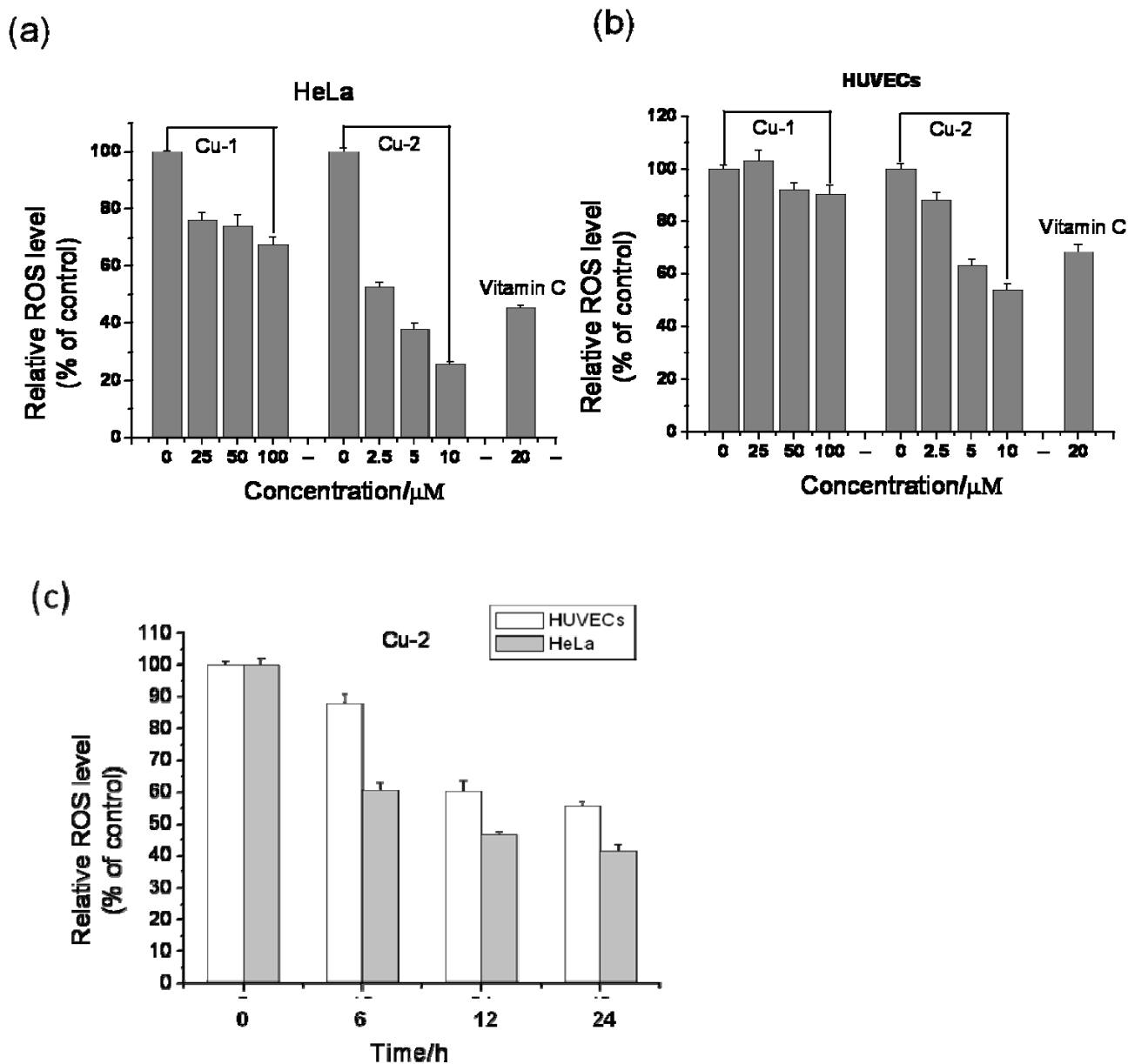


Fig. S10 Effects of Cu-1, Cu-2 and vitamin C on ROS levels in HeLa cells or in HUVECs stained by DCFH-DA. (a) ROS levels were analysed by flow cytometry after HeLa cells were incubated with different concentrations of Cu-1 or Cu-2 and Vitamin C (20 μM) for 24 h. The ROS levels decreased as concentration increased in HeLa cells. (b) ROS levels were analysed by flow cytometry after HUVECs were incubated with different concentrations of Cu-1 or Cu-2 and Vitamin C (20 μM) for 24 h. The ROS levels also decreased as concentration increased in HUVECs. (c) ROS levels were analysed by flow cytometry after HUVECs or HeLa cells were incubated with Cu-2(5 μM) for 0, 12, 24 and 48 h, respectively. The ROS levels decreased as time increased. After the cells were incubated with Cu-2(5 μM) for 24 h, the ROS levels were lower than those of vitamin C (20 μM). The experiment was performed in three independent experiments, and the results were expressed as mean \pm SD.

References

1. K. E. Koenig, C.M.Lein , P. Stuckler , T. Kaneda and D. J. Cram, *J. Amer. Chem. Soc.* 1979, **101**, 3553.
2. S. Taniguchi, *Bull. Chem. Soc. Jpn.* 1984, **57**, 2683.
3. X. Y. Qin, S. H. Zhang, Y. M. Jiang , J. C. Liu and J. H. Qin, *J. Coord. Chem.*, 2009, **62**, 427.
4. Bruker SMART (Version 5.051), SAINT (Version 5.01) and SADABS (Version 2.0). Bruker AXS Inc., 1998, Madison, Wisconsin, USA.
5. G. M Sheldrick, *Acta Cryst. A.* 2008, **64**, 112.
6. O. V. Dolomanov, L. J. Bourhis, R. J. Gildea, J. A. K. Howard and H. Puschmann, OLEX2: a complete structure solution, refinement and analysis program. *J. Appl. Cryst.* 2009. **42**, 339.